# Sintering Ability of Y-Doped $BaZrO_3$ Refractory with Nano-$CaCO_3$ and the Interaction with $Ti_2Ni$ Alloys


**Baobao Lan, Wang Shihua, Yubin Xiao, Xionggang Lu, Guangyao Chen and Chonghe Li**

**Abstract** In this work, the effect of nano-$CaCO_3$ additive on the sinter-ability of Y-doped $BaZrO_3$ refractory and its interaction with $Ti_2Ni$ alloys was studied. The results showed that no second phase was observed in the Y-doped $BaZrO_3$ refractory with nano-$CaCO_3$ additive after sintering at 1750 °C for 6 h. The nano-$CaZrO_3$ promoted the densification and the growth of grains of Y-doped $BaZrO_3$ refractory. The relative density of Y-doped $BaZrO_3$ refractory with nano-$CaCO_3$ addition was about 97.5%. The melting experiment of $Ti_2Ni$ alloys was performed in the Y-doped $BaZrO_3$ crucible with nano-$CaCO_3$ additive at 1650 °C for 5 min, 10 min, and 15 min, respectively. Interaction analysis indicated that the thickness of the erosion layer was 2635 um, 3090 um, and 3689 um, respectively; and the content of oxygen was 0.412 wt%, 0.584 wt%, and 1.140 wt%, respectively.

**Keywords** Y-doped $BaZrO_3$ · $Ti_2Ni$ · Interface reaction

## Intruduction

Titanium alloys have been paid more attention due to their low density, high specific strength and corrosion resistance and for biomedical applications because of their good biological performance [1–4]. The high production cost of titanium

B. Lan · Y. Xiao · X. Lu · G. Chen (✉) · C. Li
State Key Laboratory of Advanced Special Steel, Shanghai Key Laboratory of Advanced Ferro Metallurgy, School of Materials Science and Engineering, Shanghai University, Shanghai, China
e-mail: cgybless1@shu.edu.cn

X. Lu · C. Li (✉)
Shanghai Special Casting Engineering Technology Research Center, Shanghai, China
e-mail: chli@staff.shu.edu.cn

W. Shihua
Shanghai University, Shanghai, China



B. Li et al. (eds.), *Advances in Powder and Ceramic Materials Science*,
The Minerals, Metals & Materials Series,
https://doi.org/10.1007/978-3-030-36552-3_14

alloys has limited their application. Vacuum induction melting in a refractory crucible is a lower cost production of titanium alloys compared to the conventional induction skull melting in a water-cooled copper crucible. However, the alloy melts with high chemical activity and can easily react with the refractory to contaminate the melts indicating that the refractory should possess the high thermodynamic stability to resist the erosion by the melt. Molten titanium alloys will react with common refractories such as $SiO_2$, MgO, BN, $Al_2O_3$. Kartavykh [5] melted Ti–Al-Nb alloy in the BN crucible. A significant interaction occurred between the BN crucible and the molten alloy, and a layer of reactants was attached to the side of the alloy. Frenzel et al. [6] found that the graphite crucible could easily react with the NiTi alloy melt at high temperature as well as the generation of TiC reactant. Economos and Kingery [7] used the $ZrO_2$ crucible to melt pure titanium alloys. The generation of TiO appeared after melting. Weber [8] used MgO crucible to melt the pure titanium alloy. An obvious interaction region was observed in the crucible side. Calcium oxide was a stable refractory with a low price. However, CaO crucible is easy to hydrate in the air, which would cause the melt contamination by the increase of oxygen concentration during the melting process. $Y_2O_3$ had higher stability than that of CaO, and the $Y_2O_3$ crucible was widely used in titanium casting and directional solidification of TiAl alloy. For melting TiAl alloys, the $Y_2O_3$ crucible exhibited better corrosion resistance than that of CaO, $ZrO_2$, and $Al_2O_3$ crucibles [9]. However, the thermal shock resistance of $Y_2O_3$ crucible was poor and serious breakage would occur after several times of use, which could not realize repetitive use and cause great waste.

Recently, the perovskite compound ($CaZrO_3$ and $BaZrO_3$) was introduced as the refractories for melting titanium alloys because of their high melting point and chemical stability. Zhang et al. [10] melted the NiTi alloy with the $BaZrO_3$ crucible. It was found that the molten alloy did not react with the crucible refractory and the oxygen content of the alloy was only 450 ppm; no refractory elements were found in the alloy. Zhou [11] used the $BaZrO_3$ crucible to prepare the TiFe-based hydrogen storage alloy, which has the hydrogen storage performance and was not weaker than graphite as well as no contamination of carbon. In addition, Chen et al. [12, 13] found that the high titanium content of alloys would react with the $BaZrO_3$ refractory because of the dissolution of $BaZrO_3$ in the titanium alloy melts, and severe damage of the $BaZrO_3$ crucible would happen. Currently, doping is a simple and potentially effective method to improve the stability of $BaZrO_3$, the oxide, such as $In_2O_3$ [14] and $Y_2O_3$ [15], which are the common additives. Due to the high activity of titanium melts, some additives, such as the $In_2O_3$ and $Bi_2O_3$, can react with and contaminate the melts, obviously, they should be excluded as the additives for melting titanium alloys. $Y_2O_3$ exhibits sufficient stability to titanium melts and implies that it may be an appropriate additive. Kang et al. [16] revealed that the stability of $BaZrO_3$ refractory could be improved by doping $Y_2O_3$, and the Y-doped $BaZrO_3$ crucible exhibited a better performance than that of the $BaZrO_3$ crucible after melting the $Ti_2Ni$ alloys. Meanwhile, Chen [17] presented that the CaO also was a good additive to improve the stability of the $BaZrO_3$ refractory. However, the effects of nano-$CaCO_3$ additive into Y-doped $BaZrO_3$ and the interface reaction

between Y-doped $BaZrO_3$ crucible with nano-$CaCO_3$ additive and titanium-rich alloys have not been reported.

In this paper, the BZY was doped with 10 mol% nano-$CaCO_3$ for melting $Ti_2Ni$ alloy. The experimental process was smelting $Ti_2Ni$ alloy at 1650 °C for 5 min, 10 min, and 15 min, respectively. The relationship between the thickness of the crucible reaction layer and the smelting time at 1650 °C was studied.

## Experiment

First, the industrial grade $BaCO_3$, $ZrO_2$, and $Y_2O_3$ were selected according to the molar ratio n($BaCO_3$): n($ZrO_2$): n($Y_2O_3$) = 1: 0.97: 0.015 for preparing the $BaZr_{0.97}Y_{0.03}O_3$ (BZY) refractory. Then, the powder was mixed in a ball mill for 8 h in a ratio of mass ratio m (powder): m (ball mill beads): m (alcohol) = 2: 3: 0.4, so that they were thoroughly mixed. And the BZY powder was made by reacting the corresponding oven-dried mixtures at 1400 °C for 12 h. Next, the BZY refractory was doped with 10 mol% nano-$CaCO_3$, and the powder was mixed in a ball mill for 8 h to obtain nano-$CaCO_3$-doped BZY (BZY–Ca); the distribution of the powders is shown in Table 1. The powder mixtures were fabricated into the crucibles in a U-shape steel mandrel of 3.5 cm width and 4.5 cm height by using the cold isostatic pressing with a pressure of 120 MP for 3 min and sintered with dwell times of 3 h and 6 h at 1450 °C and 1750 °C, respectively. The crucible after sintering had a width of 2.9 cm and a height of 3.7 cm. A slow heating rate was controlled at 2 °C/min to avoid the generation of cracks.

The objective of our melt trials was to produce $Ti_2Ni$ ingot. High purity raw Ni sheet (> 9.99%) and sponge titanium (> 9.9%) were used as the raw materials. Before the melting, the crucible was placed in the VIM furnace and then backfilled with MgO ramming mass to prevent damage of the induction coil in case of crucible failure. The raw material ingredients were placed in the crucible and the furnace was evacuated to $10^{-3}$ Pa and backfilled with high purity argon gas for at least three times, in order to isolate the effect of the oxygen pickup exclusively from the chamber. Then the melting was performed under the high vacuum. Once the melt was visible, backfilled the argon gas quickly and raised gradually the temperature up to 1650 °C, and kept at this temperature for 5 min. Then the melt was poured into the graphite crucible and cooled in the furnace. The experiment of melting $Ti_2Ni$ alloys for 10 and 15 min was followed by the same procedure, respectively.

**Table 1** the mole ratio of $BaCO_3$, $ZrO_2$, $Y_2O_3$ and nano-$CaCO_3$ for preparing the BZY–Ca

| | $BaCO_3$ | $ZrO_2$ | $Y_2O_3$ | Nano-$CaCO_3$ |
|---|---|---|---|---|
| BZY–Ca | 1 | 0.97 | 0.015 | 0.01 |

The phase identification was conducted by X-ray diffraction (XRD, D8 advance, Bruker) using nickel filtered CuKa radiation. The sidewall of the crucible after melting was investigated using the scanning electron microscope (JSM-6700F). To evaluate the melt contamination of TiAl alloy by the crucible refractory, the alloy was investigated by inductively coupled plasma atomic emission spectrometry (ICP-AES). During the sample preparation, an about 10 mm thick ingot was first removed from the alloy by wire-electrode cutting, then, 0.1 g samples were obtained by abrasive cutting, and washed in the hydrofluoric acid for ICP-AES. Overall oxygen content in the alloy was measured by LECO TC600 O/N analyzer.

## Results and Analysis

The densities of the crucibles with nano-$CaCO_3$ additives were determined by full automatics density analyzer (ACCUPYC II 1340). And the density of BZY–Ca crucible is 5.94 g/cm$^3$, while the theoretical density (6.09 g/cm$^3$) of Y-doped $BaZrO_3$ with nano-$CaCO_3$ is calculated by the weighted average method [17], the relative density of BZY–Ca crucible is 97.9%. The XRD patterns of the BZY powder and BZY–Ca powder were shown in Fig. 1. The reflections for BZY powder was well indexed with cubic symmetry (Pm-3m) about ICDD data for $BaZrO_3$ [PDF-06-0399]. No traces of second phase were found indicating the substitution of Y at lattice sites of $BaZrO_3$ matrix. Meanwhile, the degree of peak shift of nano-$CaCO_3$-doped BZY (BZY–Ca) refractory appeared. It was because that a shrinkage of $BaZrO_3$ lattice (d-value) after doping the Ca ion would happen due to the smaller atomic radius of $Ca^{2+}$ (0.1 nm) compared with that of $Ba^{2+}$ (0.135 nm). According to the Bragg's law: $2d\sin\theta = n\lambda$, the decreasing of d-value will lead to the increasing of the θ-value.

Figure 2 presents that the second electron (SE) and backscattered electron (BSE) images for the BZY–Ca pellets. No second phase was observed in the

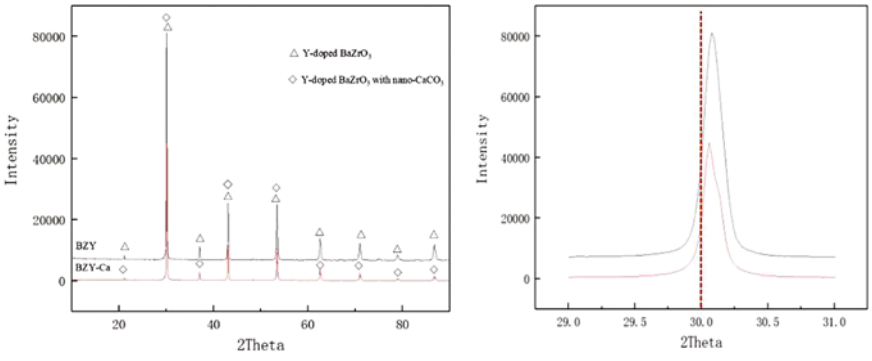


**Fig. 1** XRD spectra for the nano-$CaCO_3$-doped BZY refractory

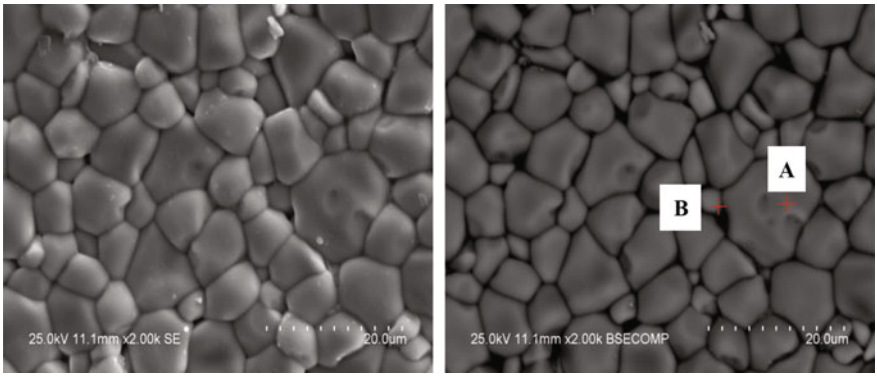


**Fig. 2** The second electron (SE) and backscattered electron (BSE) images for the BZY–Ca pellet

BZY–Ca pellet by combining with the XRD spectra in Fig. 1. Apparently, the Ca element could solute into the BZY refractory. Combined with the result of the EDS of the crucible, it can be concluded that the pellet was contained only the BZY–Ca phase (Table 2).

The $Ti_2Ni$ alloy was melted in the BZY–Ca crucibles at 1650 °C for 5 min, 10 min, and 15 min, respectively. The morphology and corrosion of the crucibles after smelting was shown in Fig. 3. Finally, the contamination of the alloy after different smelting times was investigated. As the melting time was increased, the corrosion degree of the crucible by the alloy melt was also gradually increased. As shown in Fig. 3, the thickness of corrosion layer is 2635 um, 3090 um, and 3689 um, when the melting time was 5 min, 10 min, and 15 min, respectively. The contents of Zr, Ba, Ca, O elements in the alloy were shown in Table 3. From the Table 3, the impurities in the $Ti_2Ni$ alloys were also increased with the increasing melting time. The content of oxygen was increasing from 0.412 wt% to 1.14 wt%. Kang [18] presented that the dissolution of Y-doped $BaZrO_3$ refractory in the titanium alloy melt was the main responsibility for the corrosion of the crucible refractory. Apparently, the Y-doped $BaZrO_3$ refractory with nano-$CaCO_3$ additive also exhibited a high thermodynamic stability to the titanium alloy melts. Although the inside of the crucible was eroded, the morphology of the crucible was also retained. Meanwhile, the dissolution content of the refractory was increased with the increasing melting time. According to the previous study in our group, the $BaZrO_3$ refractory could be dissolved in the titanium melts leading to the erosion of

**Table 2** The EDS results of point A and B in Fig. 2

| Position | Element/at. % | | | | | Possible phase |
|---|---|---|---|---|---|---|
| | Ba | Ca | Zr | O | Y | |
| A | 31.38 | 4.17 | 29.29 | 31.58 | 3.59 | $Ba_xCa_{1-x}Zr_yY_{1-y}O_3$ |
| B | 32.59 | 4.14 | 29.32 | 30.35 | 3.60 | $Ba_xCa_{1-x}Zr_yY_{1-y}O_3$ |

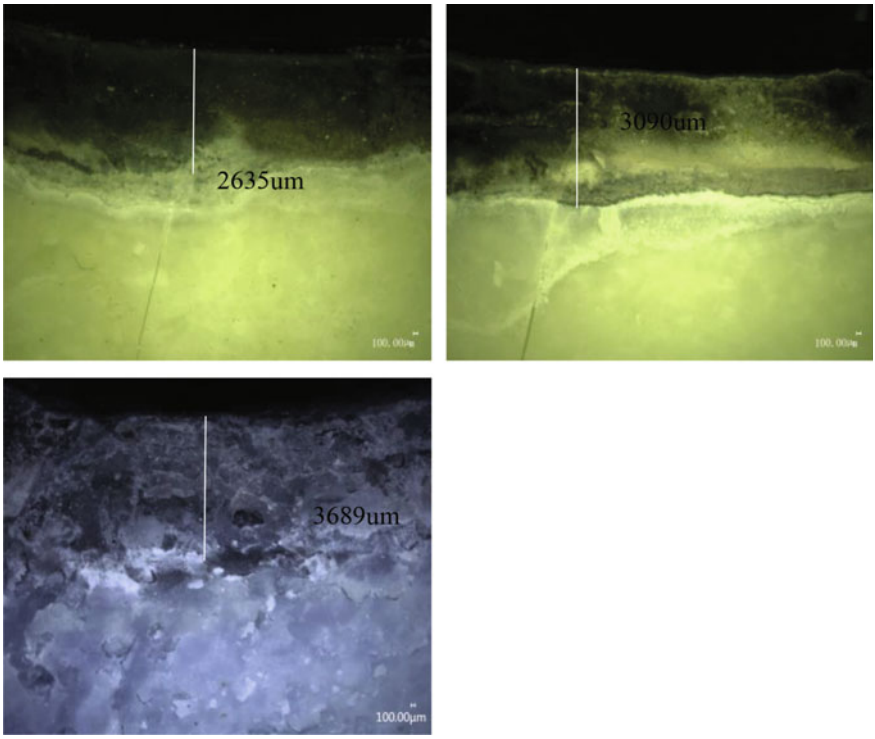


**Fig. 3** The macro picture of the corrosion layer of the crucible after melting at 1650 °C for 5 min, 10 min and 15 min respectively **a**: 5 min; **b**: 10 min; **c**: 15 min

**Table 3** The concentration of impurities in the $Ti_2Ni$ alloy after melting

| | Time | Ba (ppm) | Zr (wt%) | Ca (wt%) | O (wt%) |
|---|---|---|---|---|---|
| BZY–Ca | 5 | 18 | 0.85 | 0.019 | 0.414 |
| | 10 | 16 | 1.14 | 0.018 | 0.584 |
| | 15 | 6 | 1.07 | 0.019 | 1.14 |

the refractory [19], Kang [20] used BZY crucible to melt $Ti_2Ni$ alloy and found that the crucible does not react with $Ti_2Ni$ alloy; it may be caused by decomposition of refractory. Y-doped $BaZrO_3$ refractory and Ca-doped $BaZrO_3$ refractory will dissolve in the titanium melt, and dissolve erosion process is directly related to the Gibbs free energy of formation for the refractory; the Gibbs free energy of formation for the $BaZrO_3$ refractory could decline further with Ca and Y co-additive, so the dissolution of Ca–Y doped $BaZrO_3$ refractory will occur in the process of titanium melting.

## Conclusion

(1) No secondary phase was observed in the Y-doped $BaZrO_3$ refractory with nano-$CaCO_3$ additive, and the refractory was a cubic perovskite structure. Besides, the relative density of the crucible was 97.8%.
(2) After melting the $Ti_2Ni$ alloy at 1650 °C for 5 min, 10 min, and 15 min, respectively, the thickness of the erosion layer of the crucible was 2635 um, 3090 um, and 3689 um, respectively.

**Acknowledgements** The authors thank the National Natural Science Foundation of China-CHINA BAOWU STEEL GROUP Joint research fund for iron and steel (No.: U1860203, U1860108); National Natural Science Foundation of China (No.: U1760109); Scientific research innovation project of Shanghai education commission (No.:15ZS030).

## References

1. Wang X D, Lu FS, Jia H, et al(2014) Titanium industry development report of China in 2013. China's Titanium Industry 21(1):30–36 (in Chinese)
2. Wu X (2006) Review of alloy and process development of TiAl alloys. Intermetallic 14 (10):1114–1122
3. Boyerr RR (1996) An overview on the use of titanium in the aerospace industry. Mater Sci Eng A 213(1–2):103–114
4. Niinomi M, Boehlert CJ (2006) Titanium alloys for biomedical applications. Mater Sci Eng C 26(8):1269–1277
5. Kartavykh AV, Tcherdyntsev VV, Zollinger J (2009) TiAl–Nb melt interaction with AlN refractory crucibles. Mater Chem Phys 116(1):300–304
6. Frenzel J, Zhang Z, Neuking K et al (2004) High quality vacuum induction melting of small quantities of NiTi shape memory alloys in graphite crucibles. J Alloy Compd 385(1):214–223
7. Economos G, Kingery WD (2010) Metal-ceramic interactions: ii, metal-oxide interfacial reactions at elevated temperatures. J Am Ceram Soc 36(12):403–409
8. Weber BC, Thompson WM, Bielstein HO et al (2010) Ceramic crucible for melting titanium. J Am Ceram Soc 40(11):363–373
9. Tetsui T, Kobayashi T, Mori T et al (2010) Evaluation of yttria applicability as a crucible for induction melting of TiAl alloy. Mater Trans 51(9):1656–1662
10. Zhang Z, Zhu KL, Liu LJ et al (2013) Preparation of $BaZrO_3$ crucible and its interfacial reaction with molten titanium alloys. J Chin Ceram Soc 41(9):1278–1283 (in Chinese)
11. Li CH, Zhou H, Chen GY et al (2016) Preparation of TiFe based alloys melted by $BaZrO_3$ crucible and its hydrogen storage properties. J Chongqing Univ 39(2):107–113 (in Chinese)
12. Chen GY, Cheng ZW, Wang SS et al (2016) Interfacial reaction between high reactivity titanium melt and BaZrO3 refractory. J Chin Ceram Soc 44(6):890–895
13. Chen GY, Li BT, Zhang H et al (2017) Corrosion mechanism of BaZrO3 refractory in titanium enrichment melt. Chin J Nonferrous Metals 27(5):947–952
14. Bi L, Fabbri E, Sun Z et al (2011) Sinteractivity, proton conductivity and chemical stability of $BaZr_{0.7}In_{0.3}O_{3-\delta}$ for solid oxide fuel cells (SOFCs). Solid State Ion 196(1):59–64
15. Reddy GS, Bauri R (2016) Y and In-doped BaCeO3–BaZrO3 solid solutions: chemically stable and easily sinterable proton conducting oxides 688:1039–1046
16. Kang JY, Chen GY, La BB et al (2018) Preparation of high density $BaZr_{0.97}Y_{0.03}O_{3-\delta}$ ceramic and its interaction with titanium melt. Key Eng Mater 768:261–266

17. Chen GY, Kang JY, Gao PY et al (2018) Effect of CaO additive on the interfacial reaction between the $BaZrO_3$ refractory and titanium enrichment melt. Rare metal technology 2018. In: The minerals, metals & materials series. https://doi.org/10.1007/978-3-319-72350-1_22
18. Kang JY, Chen GY, Lan BB et al (2019) Stability of Y-doped $BaZrO_3$ and resistance to titanium melt. Chin J Nonferrous Metals 29(4):749–754 (in Chinese)
19. Chen GY, Kang JY, Gao PY et al (2018) Dissolution of $BaZrO_3$ refractory in titanium melt[J]. Int J Appl Ceram Technol. https://doi.org/10.1111/ijac.13009
20. Kang JY, Chen GY, Lan BB et al (2019) Sintering behavior of Y-doped BaZrO3 refractory with TiO2 additive and effects of its dissolution on titanium melts[J]. Int J Appl Ceram Technol 16(3):1088–1097